Proceedings of IMECE2002
ASME International Mechanical Engineering Congress & Exposition
November 17–22, 2002, New Orleans, Louisiana

IMECE2002-33075

NUMERICAL ANALYSIS OF THE HYDRODYNAMICS OF THE FLOW IN AN AXIALLY ROTATING HEAT PIPE

Gustavo Gutierrez
Mechanical Engineering Department
University of Puerto Rico
Mayaguez, Puerto Rico 00681-9045

Tien-Chien Jen
Mechanical Engineering Department
University of Wisconsin, Milwaukee
Milwaukee, WI 53211

ABSTRACT

A numerical study is conducted on the vapor and liquid flow in a wick structure of an axially rotating heat pipe. For the vapor, the governing equations are the Navier-Stokes. For the liquid a space average of the Navier-Stokes equation is performed and a porous media model is introduced for the cross correlation that appears from the averaging process. A control volume approach on a staggered grid is used in the development of the computer program. Suction and blowing velocities are used as boundary conditions of the vapor and liquid, which are related to a local heat flux input in the evaporator section, and local heat flux output in the condenser section, respectively. The aim behind this study is the application of heat pipes in drilling applications. A triangular heat flux distribution is assumed in the evaporator due to the higher heat flux generated at the tip of the drill. A parametric study is conducted to analyze the effect of different parameters such as rotational speeds, saturation conditions, porosity, permeability and dimensions of the wick structure in the porous medium. These parameters significantly affect the pressure drop in the heat pipe and allow predicting failure conditions, which is critical in the design of heat pipes in drilling applications. The results of this study will be useful for the complete analysis of the heat pipe performance including the solution of the heat transfer on the solid wall as a conjugate problem.

INTRODUCTION

Heat pipes are passive devices that can transport thermal energy with relatively low temperature difference. There is and extensive literature dedicated to heat pipes. A detailed literature review on the-state-of-art development in heat pipes can be found in Faghri [7] and Peterson [15]. However, rotating heat pipes with a wick structure has not received adequate attention. Most previous investigation in rotating heat pipes has used a Nusselt-type analysis for the liquid film (wickless heat pipes) [2, 4, 5, 9, 11]. Peterson and Wu [16] present a review of rotating and revolving heat pipes. They indicate that the performance of rotating heat pipes without an internal taper is mainly affected by rotating speed, working fluid fill ratio, properties of the working fluid, working temperature, inclination angle and wick structure. In rotating heat pipe with an internal taper, the rotational speed was found to be the most significant parameter. Daniels and Al-Jumaily [5] carried out an investigation of the factors affecting the performance of a rotating heat pipe. The authors performed a theoretical analysis of the condensation process using a Nusselt-type approach. Their analytical results were validated with experimental data for rotational speed between 600 and 1200 rpm. They concluded that the rotational speed enhances the heat transfer capability, but the rate of increase of heat transfer tends to decline indicating an upper speed limit. However, for a heat pipe with a wick structure, the physical mechanism of heat transfer is different and it is not clear what is the effect of the rotational speed on heat pipe performance. Sobhan *et al.* [17] solved the conjugate problem for the vapor, wick structure and solid wall for a flat heat pipe, using the volume-averaged of the Navier-Stokes equation in the porous media. However, in a rotating heat pipe, additional couplings are introduced and the momentum equation in the circumferential direction has to be solved as well. The extra terms, which come from Coriolis acceleration, create numerical instability that has to be treated carefully. For parametric studies, an efficient code is desirable to obtain results at relative low cost in CPU time. Most of previous numerical works reported in the literature do not give enough attention to the numerical efficiency. Faghri *et al*. [8] use a line-by-line TDMA iteration in the axial direction and the Jacobi point-by-point in the radial direction. Sobhan *et al.* [17] use a line-by-line TDMA iteration and a very fine time step for the transient calculation. Issaci *et al.* [12] used a SOR method

which is more time consuming. These solvers propagate the boundary condition information at a very slow rate and usually require a long time to get convergence. Here, a conjugate gradient stabilized method (CGSTAB) proposed by Van der Vorst and Sonnevald [18] is used. This method has shown an excellent performance when it was compared with line-by-line TDMA, ADI and SIP methods. The formulation was carried out in a way that allows using the same code for the vapor and the liquid flow solving the Navier-Stokes equations. In this study, an incompressible, laminar and axisymmetric flow is assumed. For the liquid, a space average of the Navier-Stokes equations is performed and a porous media model is introduced for the cross correlation that appears from the averaging process [1]. In this study, the solution of the hydrodynamics of the flow is analyzed in detail. The heat transfer problem is uncoupled assuming input velocity profiles in the evaporator and condenser section. The reason behind this is the fact that the hydrodynamics is the most demanding numerical part and deserves more attention to improve the efficiency of the numerical code. If constant thermal properties are assumed, the energy equation will be uncoupled of the momentum equations, or better said, it will be coupled through the interface condition (i.e., through Clayperon equation). However, this coupling is not very strong because the temperature drop is very small along the vapor-liquid interface of the pipe and the velocities in the porous media are very small too. The result of this study will be beneficial for these further and more complete analyses considering the heat transfer problem in the wall of the heat pipe, which is pertinent to the drilling applications.

NOMENCLATURE

C_F : Ergun's constant, 0.55
h_{fg} : latent heat of vaporization [J/kg]
K : permeability of the porous medium [m^2]
L_e : length of the evaporator [m]
L_a : length of the adiabatic region [m]
L_c : length of the condenser [m]
p : pressure [Pa]
P_{sat} : saturation pressure [Pa]
$q(z)$: local rate of heat transfer per unit length [W/m]
Q_{total}: total amount of heat entering and leaving the heat pipe in [W] $Q_{total} = \int_A q(z)\, dA$
R_0 : radius of the heat pipe [m]
R_v : gas constant for the vapor [J/(kg K)]
Re : radial Reynolds numbers, $\mathrm{Re} = \rho V_w R_0 / \mu$
r_c : pore radius of the wick structure [m]
r, θ, z : radial, circumferential and axial coordinates
S_ϕ : source term in the generic property ϕ
t_w : thickness of the wick structure [m]
T_{sat} : saturation temperature [ºC]
V_r, V_θ, V_z : reduced velocities in the r, θ, and z direction respectively [m/s]
V_w : reduced blowing and suction velocity at the condenser and evaporator respectively [m/s]
v_i : actual velocity in the "i" direction in the microchannel of the porous medium [m/s]
$\bar{v}_i$: average velocity within the void space of the porous medium [m/s]
v_i' : local spatial deviation in the "i" direction within the void space [m/s]
$\bar{V}_i$: Darcy velocity in the "i" direction [m/s]

Greek

ε : porosity
ρ : density [kg/m^3]
σ : surface tension [N/m]
ϕ : generic property
μ : dynamic viscosity [kg/(m s)]
Γ : diffusivity for the generic property ϕ
Ω : angular velocity [rad/s]

THE PHYSICAL MODEL

In this paper, attention is focused on the hydrodynamics of the flow of a rotating heat pipe. The aim behind this study is the application of heat pipes in drilling applications. To uncouple the conjugate heat transfer problem in the pipe wall, an assumption is needed about the heat flux input at the evaporator section and the heat flux output at the condenser section, which is related to the blowing and suction flow conditions at these sections. It is assumed that a triangular heat flux distribution at the evaporator and a uniform heat flux distribution at the condenser. This triangular heat flux distribution is a reasonable assumption because higher heat fluxes are generated at the tip of the drill. Figure 1 shows the physical domain for the vapor and for the wick structure and the coordinate system of a rotating heat pipe. The basic geometric configuration of the heat pipe and parameters are summarized in the Table 1. The thermal physical properties of the working fluid (water, in this study) play an important role in the determination of the capillary limit. These properties are summarized in Table 2. Some parametric studies are conducted to analyze the effect of different rotating speeds, saturation conditions, porosity, permeability and dimension of the wick structure. A pore radius r_c of approximately 3.2×10^{-5} meters has been used to calculate the capillary pressure, $\Delta P_c = 2\,\sigma / r_c$.

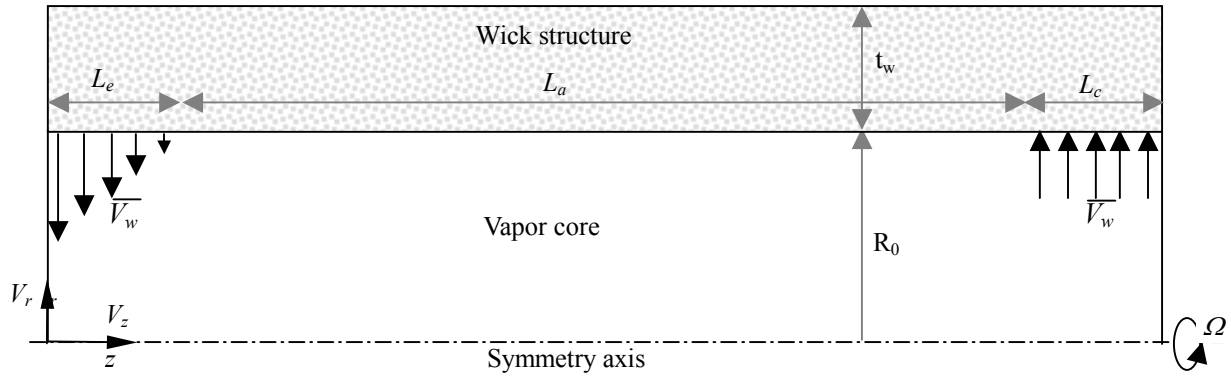

Figure 1 – Physical domain and coordinates

Table 1: Basic geometric configuration and parameters of the heat pipe

Le	0.025 m	R_0	0.0075 m	R_v	0.4615 KJ/(kg K)
La	0.15 m	t_w	0.001 m	ε	*0.5*
Lc	0.025 m	Q_{total}	85 W	*K*	$1.4\ 10^{-11}\ m^2$

Table 2: Thermo physical properties of water

	50 °C	75 °C	100 °C	125 °C	150 °C
h_{fg} *(kJ/kg)*	2.383E+03	2.320E+03	2.255E+03	2.188E+03	2.114E+03
ρ_l *(kg/m^3)*	9.884E+02	9.750E+02	9.585E+02	9.391E+02	9.170E+02
ρ_v*(kg/m^3)*	8.295E-02	2.418E-01	5.975E-01	1.298E+00	2.547E+00
μ_l *(kg/(m s))*	5.440E-04	3.742E-04	2.791E-04	2.201E-04	1.810E-04
μ_v *(kg/(m s))*	1.008E-05	1.111E-05	1.208E-05	1.298E-05	1.385E-05
σ *(N/m)*	6.779E-02	6.354E-02	5.892E-02	5.392E-02	4.867E-02

MATHEMATICAL FORMULATION

The evaporation and condensation are considered uniform around the circumferential direction. Based on this assumption, the problem becomes axis-symmetric and all the derivatives with respect to the circumferential direction are zero. Thus, the problem becomes two-dimensional in cylindrical coordinates. However, in axis-symmetric swirling flow the momentum equation in the circumferential direction has to be solved as well. The vapor and liquid flow are assumed laminar and incompressible. For the vapor core the Navier-Stokes equations apply. For the liquid flow, the conceptual model is a porous medium. In porous media, the Navier-Stokes equations are still valid but only for each fluid element inside the micro channel. However, due to the complex geometric configuration, the flow becomes very complicated and some kind of averaging is necessary to make the problem more treatable mathematically. This idea is in some way similar to the time-averaging approach in turbulent flow. In porous media instead, a space averaging process is performed as (Bear, [1]):

$$v_i = \overline{v}_i + v'_i \qquad (1)$$

where v_i is the actual velocity in the "*i*" direction, $\overline{v}_i$ is the average velocity within the void space and v'_i is a local spatial deviation in the "*i*" direction within the void space. The cross products that appear from the average process can be expressed as:

$$\overline{v_i v_j} = \overline{v}_i \overline{v}_j + \overline{v'_i v'_j} \qquad (2)$$

For *i=j,* $\overline{v'^2_i}$ is the variance and for $i \neq j$ $\overline{v'_i v'_j}$ is the covariance of the velocity distribution. The actual execution of the averaging process to obtain $\overline{v}_i$ and v'_i is impossible

without information about the real distribution of v_i within the void space in a representative control volume. Since we are interested only in a measurable mean values, some general assumption regarding to the correlation between the velocities v_i and v_j are needed. If it is assumed that these variables are independent of each other, then the covariance $\overline{v'_i v'_j}$ will be zero. The only term that remains is the variance that, it will require some kind of modeling similar to the closure problem in turbulence. Now, performing the space-averaging process to the Navier-Stokes equations:

$$\frac{\partial(\rho \bar{v}_i \bar{v}_j)}{\partial x_j} = -\frac{\partial \hat{p}}{\partial x_i} + \frac{\partial}{\partial x_j}\left(\mu \frac{\partial \bar{v}_i}{\partial x_j}\right) - 2\rho\Omega \times \bar{v}_i - \rho \frac{\partial \overline{v_i'^2}}{\partial x_j}\delta_{ij} \tag{3}$$

where $\hat{p}$ is the reduced pressure

$$\hat{p} = p - \frac{1}{2}\rho\Omega^2 r^2 - \rho g h$$

Here h is the height of the heat pipe respect to the horizontal position. The average velocity $\bar{v}_i$ is related to the Darcy velocity $\bar{V}_i$ by the Dupuit-Forchheimer relationship, $\bar{V}_i = \varepsilon \bar{v}_i$, where ε is the porosity. Writing Equation (3) in terms of the Darcy velocity yields:

$$\frac{1}{\varepsilon^2}\frac{\partial(\rho \bar{V}_i \bar{V}_j)}{\partial x_j} = -\frac{\partial \hat{p}}{\partial x_i} + \frac{1}{\varepsilon}\frac{\partial}{\partial x_j}\left(\mu \frac{\partial \bar{V}_i}{\partial x_j}\right) - \frac{2}{\varepsilon}\rho\Omega \times \bar{V}_i - \rho \frac{\partial \overline{v_i'^2}}{\partial x_j}\delta_{ij} \tag{4}$$

The term $\rho \frac{\partial \overline{v_i'^2}}{\partial x_j}\delta_{ij}$ represents some kind of viscous resisting force due to the variation of the flow in the microchannels of the porous medium. At this point it is introduced the porous medium model equivalent in some way to the constitutive equations in the continuum model. It is assumed that this resistance force is proportional to the averagd velocity at that point plus an additional term proportional to the square of the velocity and they are acting in a direction opposite to the local average velocity:

$$-\rho \frac{\partial \overline{v'_i}^2}{\partial x_j}\delta_{ij} = -\frac{\mu}{K}\bar{V}_i - c_F K^{-0.5}\rho\left|\bar{V}_i\right|\bar{V}_i \tag{5}$$

where K is called the "permeability" of the porous medium and the coefficient C_F is the Ergun's constant which value is approximately 0.55. The first term on the right hand side is called the Darcy term and the second one is called the Forchheimer term. Introducing this model into Equation (4):

$$\frac{1}{\varepsilon^2}\frac{\partial(\rho \bar{V}_i \bar{V}_j)}{\partial x_j} = -\frac{\partial \hat{p}}{\partial x_i} + \frac{1}{\varepsilon}\frac{\partial}{\partial x_j}\left(\mu \frac{\partial \bar{V}_i}{\partial x_j}\right) - \frac{2}{\varepsilon}\rho\Omega \times \bar{V}_i - \frac{\mu}{K}\bar{V}_i - \frac{C_F}{K^{0.5}}\rho\left|\bar{V}_i\right|\bar{V}_i \tag{6}$$

If a "reduced velocity" $V_i = \frac{\bar{V}_i}{\varepsilon}$ is defined and is substituted in Equation (6):

$$\frac{\partial(\rho V_i V_j)}{\partial x_j} = -\frac{\partial \hat{p}}{\partial x_i} + \frac{\partial}{\partial x_j}\left(\mu \frac{\partial V_i}{\partial x_j}\right) - 2\rho\Omega \times V_i - \varepsilon\frac{\mu}{K}V_i - \varepsilon^2 \frac{C_F}{K^{0.5}}\rho\left|V_i\right|V_i \tag{7}$$

Defining a "pore Reynolds number" as:

$$\mathrm{Re}_p = \rho_l \frac{\bar{V}_i K^{0.5}}{\mu_l} \tag{8}$$

and comparing the last two terms on the right hand side of Equation (6)

$$\frac{\mu}{K}\bar{V}_i + \frac{C_F}{K^{0.5}}\rho\left|\bar{V}_i\right|\bar{V}_i = \frac{\mu}{K}\bar{V}_i(1 + C_F\,\mathrm{Re}_p) \tag{9}$$

It can be seen that if $(C_F\,\mathrm{Re}_p)$ is of order one, the Forchheimer term is of the same order as the Darcy term. Equation (7) reduces to the equation of the vapor core of the heat pipe letting ε =1 and K equal to infinity. In cylindrical coordinate and with axisymmetric condition imply that the governing equations can be written as:

Conservation of mass

$$\frac{1}{r}\frac{\partial}{\partial r}(rV_r)+\frac{\partial V_z}{\partial z}=0 \tag{10}$$

Momentum equation in the radial direction *(r -)*

$$\begin{aligned}&\frac{1}{r}\frac{\partial(\rho r V_r V_r)}{\partial r}+\frac{\partial(\rho V_r V_z)}{\partial z}=-\frac{\partial \hat{p}}{\partial r}\\&+\mu\left(\frac{1}{r}\frac{\partial}{\partial r}(r\frac{\partial V_r}{\partial r})+\frac{\partial^2 V_r}{\partial z^2}-\frac{V_r}{r^2}\right)\\&+\frac{\rho V_\theta^2}{r}+2\rho\Omega V_\theta-\varepsilon\frac{\mu}{K}V_r-\varepsilon^2\frac{C_F}{K^{0.5}}\rho V_r|V_r|\end{aligned} \tag{11}$$

Momentum equation in the circumferential direction *(θ -)*

$$\begin{aligned}&\frac{1}{r}\frac{\partial(\rho r V_\theta V_r)}{\partial r}+\frac{\partial(\rho V_\theta V_z)}{\partial z}=\\&\mu\left(\frac{1}{r}\frac{\partial}{\partial r}(r\frac{\partial V_\theta}{\partial r})+\frac{\partial^2 V_\theta}{\partial z^2}-\frac{V_\theta}{r^2}\right)-\frac{\rho V_r V_\theta}{r}\\&-2\rho\,\Omega V_r-\varepsilon\frac{\mu}{K}V_\theta-\varepsilon^2\frac{C_F}{K^{0.5}}\rho V_\theta|V_\theta|\end{aligned} \tag{12}$$

Momentum equation in the axial direction *(z -)*

$$\begin{aligned}&\frac{1}{r}\frac{\partial(\rho r V_z V_r)}{\partial r}+\frac{\partial(\rho V_z V_z)}{\partial z}=-\frac{\partial \hat{p}}{\partial z}\\&+\mu\left(\frac{1}{r}\frac{\partial}{\partial r}(r\frac{\partial V_z}{\partial r})+\frac{\partial^2 V_z}{\partial z^2}\right)\\&-\varepsilon\frac{\mu}{K}V_z-\varepsilon^2\frac{C_F}{K^{0.5}}\rho V_z|V_z|\end{aligned} \tag{13}$$

Here V_r, V_θ and V_z are the "reduced" radial, circumferential and axial velocities respectively. For the vapor, the reduced velocities are equivalent to the actual velocities. For the liquid, the actual (Darcy) velocities are the reduced velocities times the porosity, $\overline{V}_i = V_i\,\varepsilon$. Note that using this formulation, the same code to solve the flow in a two dimensional flat heat pipe can be used just letting r =1 and understanding the coordinate r as the y coordinate perpendicular to the axial direction z and setting V_θ, Ω and $\frac{V_r}{r^2}$ equal to zero.

Boundary Conditions

Since the coordinate system is fixed to the rotating pipe, at the end caps of the pipe ($z=0$ and $z=L$), the radial, circumferential and axial velocities are zero (impermeable wall and no-slip condition). The impermeable condition at the end cap near the tip can be justified by the fact that no evaporation is taking place at this end cap due to the lack of a wick structure there. At the exterior boundary of the wick structure (R_0+t_w), the radial, circumferential and axial velocities are zero (impermeable wall and no-slip condition). For the inertial frame, the non-slip condition at the walls for the circumferential velocity is $\overline{V}_\theta = \Omega r$ instead of zero as it is for the non-inertial frame. A symmetry condition is applied in the symmetric axis of the vapor core.

Evaporation and condensation at the interface of the vapor core and the wick in the evaporation and condensation region of the heat pipe are modeled as blowing and suction velocities [7] and are related to the local heat transfer rate as:

$$\overline{V}_w = \pm\frac{q(z)}{2\pi R_0\,\rho h_{fg}} \text{ and } V_w = \pm\frac{\overline{V}_w}{\varepsilon} \tag{14}$$

where $q(z)$ is the local rate of heat transfer per unit length, ρ is set to the density of the vapor when calculating the input and output velocity of the vapor core and set to the density of the liquid for the input and output velocity of the wick structure; h_{fg} is the latent heat of vaporization. The positive sign corresponds to a blowing action in the evaporator for the vapor and a suction action for the liquid; the negative sign corresponds to a suction action in the condenser for the vapor and a blowing action for the liquid (or porous media). Between the evaporator and condenser an impermeable wall condition is assumed. It is further assumed that a triangular heat flux distribution prevails at the evaporator and a uniform heat flux distribution at the condenser. This triangular heat flux distribution is a reasonable assumption in drilling applications because higher heat flux is generated at the tip of the drill. Note that, under steady state condition the amount of heat entering the pipe through evaporator section must be equal to the total heat leaving the condenser section. From this condition we can calculate the maximum velocity at the evaporator.

NUMERICAL MODELING

For the purpose of numerical analysis, it is useful to have a generic conservation equation, from which are obtained the equations of conservation of mass and momentum. This

generic conservation equation in cylindrical coordinates can be written as:

$$\frac{1}{r}\frac{\partial(\rho r V_r \phi)}{\partial r}+\frac{\partial(\rho V_z \phi)}{\partial z}=\Gamma\left(\frac{1}{r}\frac{\partial}{\partial r}(r\frac{\partial \phi}{\partial r})+\frac{\partial^2 \phi}{\partial z^2}\right)+S_\phi \quad (15)$$

where ϕ is a generic property, Γ is the diffusivity for the generic property ϕ, S_ϕ is the source term. It can be seen from Table 3 that one can reproduce the governing equations from this generic equation. The advantage of the generic conservation equation is straightforward because one has to deal with only one equation of that form in the numerical code developing. Note that the pressure gradient is included in the source term just for convenience in the notation. However, this term is treated separately since the pressure field has to be obtained as part of the solution. A pressure correction (or pressure equation) is derived from the momentum equation to enforce mass conservation. This is the basis of the SIMPLE-like algorithms [14]. The discretization in cylindrical coordinates generates additional couplings between the momentum equations as shown in Table 3. These terms are treated as extra body forces including the Coriolis force terms (i.e., $2\rho\Omega V_\theta$ and $2\rho\Omega V_r$). The term $\rho\frac{V_r V_\theta}{r}$ in the θ-momentum equation is treated implicitly when the contribution of this term to the central coefficient in the discretized equations is positive, in order to avoid instabilities of the iterative solution scheme by reducing the diagonal dominance of the matrix. Otherwise, this term is treated explicitly. The terms $\mu\frac{V_r}{r^2}$ and $\mu\frac{V_\theta}{r^2}$ in Equations (11) and (12) are treated implicitly as part of the central coefficient. For the liquid flow, the contribution of the porous media model is moved to the left hand side of the equations and treated implicitly as part of the central coefficient.

A control volume approach is used to discretize the governing equations. The diffusion terms in the generic equation are discretized using a centered difference scheme. For the convection terms a power law scheme is used. The pressure velocity coupling is solved using the SIMPLEC algorithm [19]. For details of the discretization Ferziger and Peric [6].

The Staggered Grid

The use of the staggered grid introduces a strong coupling between the velocities and the pressure that helps to avoid some convergence problems and oscillations in these fields. A typical staggered grid is shown in Figure 2. The control volumes for the axial velocity V_z and the radial velocity V_r are displaced with respect to the control volumes for the scalar variables (pressure, eventually temperature and the circumferential velocity which in axisymmetric problems do not contribute to the continuity equation and can be treated as a scalar variable). The axial velocity is calculated at the nodes defined by the coordinates X and YC. Radial velocity is calculated at the nodes defined by XC and Y coordinates and scalar variables at nodes defined by XC and YC. A variable grid is used to have a better resolution near the interface. In the axial direction the grid is generated in three zones with 16 control volumes in the evaporator and condenser zones and 50 control volumes in the adiabatic zone. The variable grid is created using an expansion coefficient, which is chosen close to unity to keep a second order accuracy. A grid independent test confirmed that this grid was good enough and was used for all the calculations.

Numerical procedure

1. Solve the V_r, and V_z momentum equations using the current values for pressure and velocities (in the first iteration a zero velocity and pressure field is assumed,

Table 3 - Terms in the generic conservation equation

ϕ	Γ	S_ϕ	Equation
1	-	0	continuity
V_r	μ	$-\frac{\partial \hat{p}}{\partial r}+\rho\frac{V_\theta^2}{r}+2\rho\Omega V_\theta$	r-momentum
V_θ	μ	$-\rho\frac{V_r V_\theta}{r}-2\rho\Omega V_r$	θ-momentum
V_z	μ	$-\frac{\partial \hat{p}}{\partial z}$	z-momentum

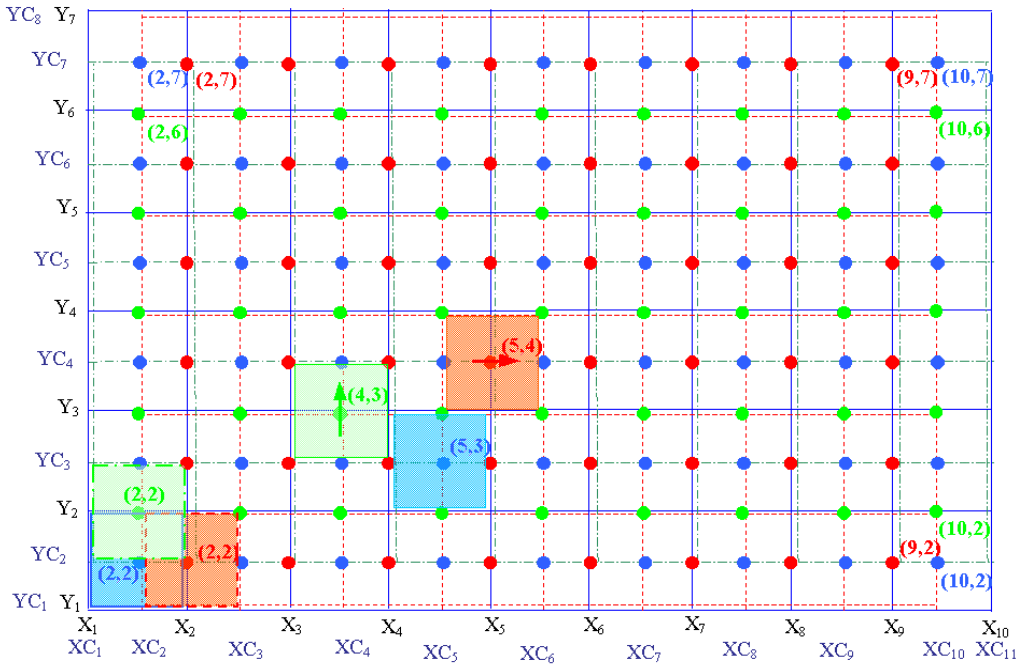

Figure 2 – A Typical Staggered Grid

except at the boundaries where the boundary conditions are applied).

2. Since the velocities obtained in Step 1 may not satisfy the continuity equation locally, the pressure correction equation is solved to obtain the necessary corrections for the velocity field (using the SIMPLEC algorithm the pressure does not need a correction).
3. Correct the velocity field until continuity is achieved.
4. Solve the V_θ momentum equation.
5. Since the momentum equations may not be satisfied with the corrected velocities, repeat steps 1 to 4 until the residual of the momentum equations and pressure equation are less than a pre-assigned convergence criterion. As for a convergence criterion, the residuals of each equation are set less than 10^{-9}.

RESULTS AND DISCUSSION

The computer program

In axisymmetric swirling flows, there are additional couplings between the radial and circumferential velocity components. Convergence problems have been reported by other authors (Gosman and Ideriah [10] and Chew [3]), for increasing rotating speeds. Gosman and Ideriah [10] suggested to add the term $\alpha\frac{\rho}{r}(\Omega r + V_\theta(V_r^{old} - V_r)$ to the radial momentum equation, where α is another form of relaxation. Unfortunately the optimum value of α is unknown and it was found in the present study any improvement in the convergence with the implementation of this term.

It is important to note that the convergence and stability improved significantly shifting the order in which the equations are solved. The best convergence was obtained solving the axial and radial momentum first, then the pressure correction and finally the circumferential velocity. In axisymmetric problems, the circumferential velocity does not contribute to the mass conservation. So, solving the pressure correction before the θ-momentum gives a velocity field that satisfy continuity and it is a better guess for the θ-momentum equation giving a much adequate convergence performance. Flow in a heat pipe with high rotational speed is highly coupled and complex and the convergence performance is strongly affected by several issues such as the numerical scheme for the convection terms, the solver used for the system of linear equations, the number of inner iterations for each outer iteration cycle, the amount of change of each variable from one iteration to the other, the under-relaxation factors, the choice of the reference frame and the initial guess of the velocity field. The selection of optimal parameters is unfortunately largely empirical. However, from numerical experiments some recommendations can be drawn with respect to some important factors that have a great impact in the convergence performance. The under-relaxation factors are one of the most important parameters for convergence. Even if different under-relaxation factors can be used for each of the momentum equations, the same relaxation factor was used for the three momentum equations (using the SIMPLEC algorithm the pressure correction does not need relaxation). For the

convection terms, two schemes were tested. The deferred correction scheme (first suggested by Khosla and Rubin, [13]) uses the following idea for the discretization of the convection terms:

$$F_{conv} = F_{conv}^{L} + \beta (F_{conv}^{H} - F_{conv}^{L})^{old} \qquad (16)$$

where F_{conv}^{L} is the approximation of the convection terms using a lower order scheme (an upwind method is used) and F_{conv}^{H} stands for the approximation using higher order scheme (centered difference is used). The superscript "old" indicates that values from previous iteration were used and β is a blending factor 0<β<1. A β=1 is used in the calculation; at convergence F_{conv}^{L} cancel out and the second order scheme remains for the convective terms. The second scheme was the power law scheme (Patankar [14]). Both algorithms have shown a good behavior for all rotational speeds. The solver used for the solution of the linear system has some impact in the convergence performance. Four different solvers, programmed in the same style, were tested: line-by-line TDMA, ADI, SIP and CGSTAB. Line-by-line TDMA and SIP needed more iterations to converge; The ADI solver shown a very good performance for its optimal parameter, comparable to the CGSTAB. The CGSTAB with ILU (Incomplete LU decomposition) as a preconditioner is chosen for all the calculations in the present work and is described in detail in reference [18].Increasing the number of inner iterations for the pressure correction equation gave better convergence performance. The number of inner iterations for each outer iteration cycle and the amount of change of each variable from one outer iteration to the next one can be programmed in a way that can be controlled as input parameters. These parameters work together as some kind of local relaxation keeping the solution smooth from one outer iteration to the other. The choice of the reference frame, inertial or non-inertial, is another factor that could impact the convergence performance. From theoretical point of view, the choice of the reference frame is irrelevant but from numerical point of view one frame could give better behavior than the other in computing the results. For the range of rotating speeds tested here, both coordinate systems gave similar convergence. In the computer program we can shift from one coordinate system to another just including the Coriolis acceleration in the source term of Equations (11) and (12) and setting the circumferential velocity $\overline{V}_{\theta} = \Omega r$ as the non-slip condition. Both must give the same results. It is important to note that these parameters are not necessarily independent of each other. However, what we expect from a robust code is obtain results that do not depend significantly on these sets of parameters. Been able to control them, can allow to obtain a more efficient code, which is very important for parametric studies.

The vapor flow

The hydrodynamics of the vapor flow at different rotating speeds and two different saturation conditions for a "radial Reynolds number Re of 25 is presented. Figure 3 shows the axial velocity profiles at the middle of the evaporation, adiabatic and condenser section for a saturation temperature T_{sat}=100°C and a total heat input of 85 W. As rotating speed increases, flow reversal is observed, turning the problem into a fully elliptic one. The maximum velocity moves from the center of the vapor core to the vapor-wick interface ($r=R_0$) generating some kind of annular main flow with a recirculating flow at the center of the pipe. Steeper gradient velocity near the interface can increase significantly the shear stresses at the interface in a wickless rotating pipe, but for a heat pipe with a wick structure it is reasonable to assume a very weak effect at the interface that in reality are not directly in contact.

In Figure 4, the same amount of heat is applied but the saturation temperature at the vapor-liquid interface is T_{sat}=50°C. It can be observed that the effect of the Coriolis force diminishes for lower saturation conditions. The lower the saturation temperature the smaller the density of the vapor and the smaller the effect of the Coriolis force. When the saturation condition decreases from 100°C to 50°C the density of the vapor changes by a factor of approximately 6, implying a similar reduction in the Coriolis force. The velocity profiles approach to the case without rotation as it is seen in Figure 4.

Figures 5 and 6 show the reduce pressure profile along the heat pipe for T_{sat}=100 °C and T_{sat}=50 °C respectively, at the centerline of the vapor core and at the liquid-vapor interface. It can be observed that a monotonically drops of the pressure in the evaporator and adiabatic sections and a pressure recovering in the condenser due to the decrease in mass flow rate, for the main flow near the interface. The pressure profile along the centerline shows a reverse pressure that generates a recirculating flow in rotating heat pipes. As seen from Figures 5 and 6, for this radial Reynolds number and dimensions of the heat pipe, the pressure drop in the vapor is very small (in the order of 1 Pa) and it is not a concern in the heat pipe design. This is not necessarily true in all situations but for the pipe analyzed here, the pressure drop in the vapor can be neglected without introducing a significant error in the estimation of the capillary limit. Performing an order of magnitude analysis and comparing the pressure drop in the vapor for laminar fully developed flow with the pressure drop in the liquid considering only the Darcy term.

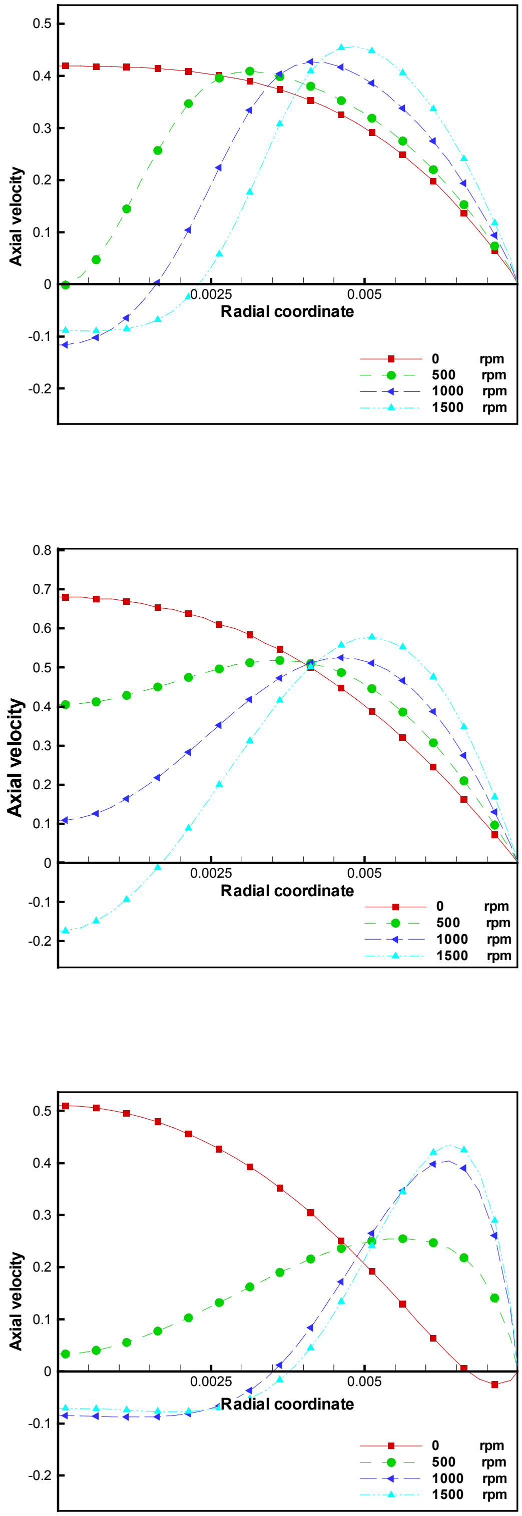

Figure 3 – Dimensionless axial velocity profiles at the middle of the evaporator (top), adiabatic region (center) and condenser (bottom) for T_{sat}= 100 °C

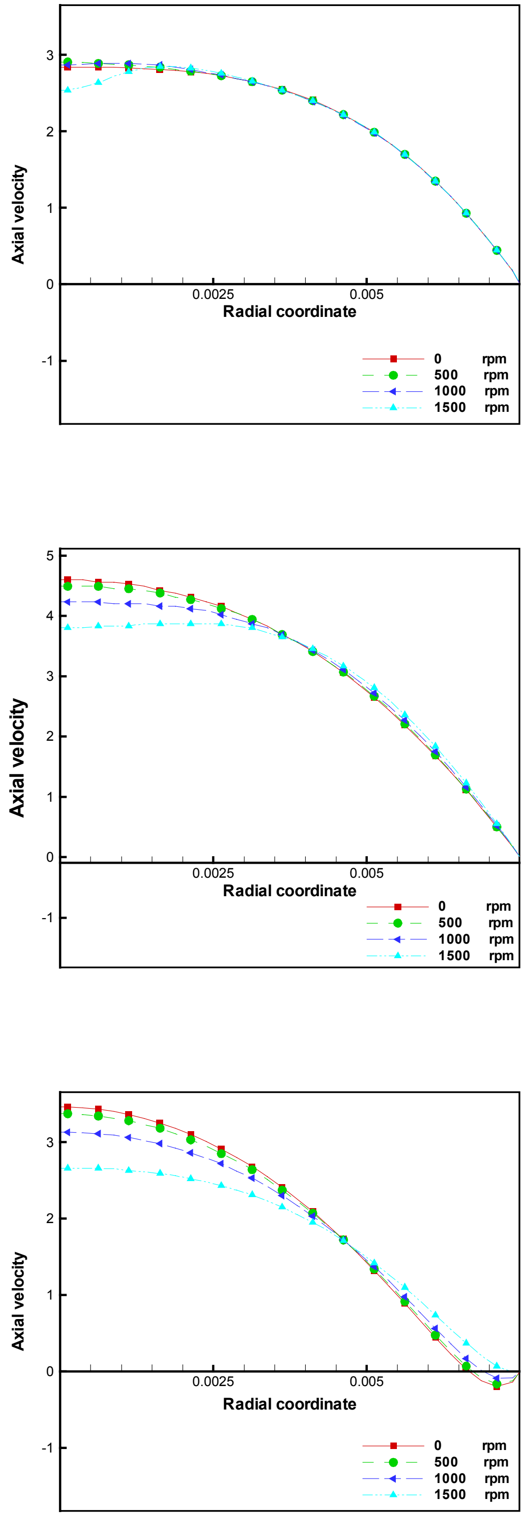

Figure 4 – Dimensionless axial velocity profiles at the middle of the evaporator (top), adiabatic region (center) and condenser (bottom) for T_{sat}= 50 °C

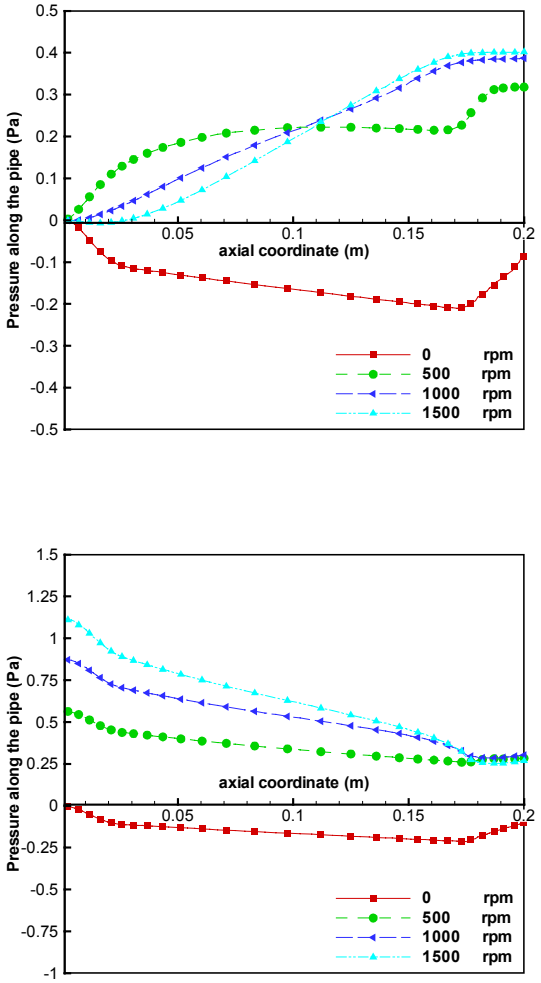

Figure 5 – Reduced pressure along the heat pipe: at the center line (top) and at the interface (bottom) T_{sat}=100 °C

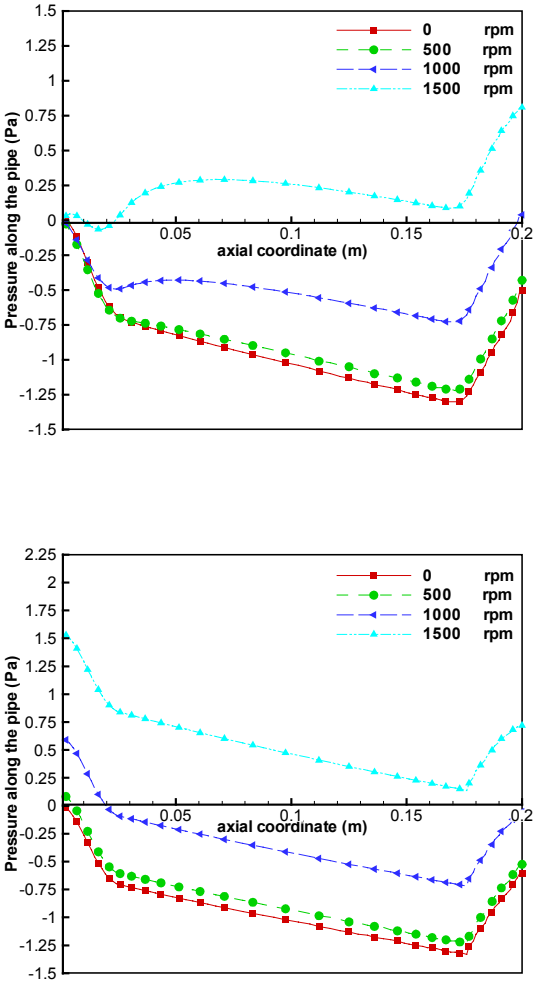

Figure 6 – Reduced pressure along the heat pipe: at the center line (top) and at the interface (bottom) T_{sat}=50 °C

It can be shown that if the term $\frac{K t_w}{R_0^3}\frac{\rho_l}{\rho_v}$ is of "order" one, the vapor pressure drop is of the same order as the pressure drop in the liquid, the pressure distribution should be considering carefully. It is important to note here that the actual pressure is the sum of the reduced pressure plus the centrifugal pressure plus the gravitational pressure. For the dimensions of the heat pipes tested in this paper, the centrifugal and the gravitational terms do not contribute significantly to the vapor pressure drop along the pipe or to the value of the pressure at the interface (e.g., for Ω=125.66 rad/s the centrifugal term ½ ρ Ω^2 R_0^2 is only 0.26 Pa).

The liquid flow

For the dimensions of the heat pipe tested here, the Forchheimer term does not have a significant influence in the velocity field. This can be easily verified numerically including the Forchheimer term in the discretization. The velocity in the adiabatic region can be very good approximation as a Darcy's velocity.

Figure 7 shows the axial velocity profiles at the middle of the evaporator, adiabatic and condenser section for a saturation temperature T_{sat}= 100 °C and a total heat input of 85 W. As seen, the velocity profiles are very uniform and completely overlap for the different rotating speeds. The rotating speeds do not have any effect in the velocity field of the porous media. The effect of saturation conditions in the liquid velocity field is not significant as it was the case of the vapor flow. However, saturation conditions have an important impact in the pressure drop of the wick.

Figure 8 shows a capillary limit curve relating the maximum transport capacity (W) versus the operating temperature (°C).

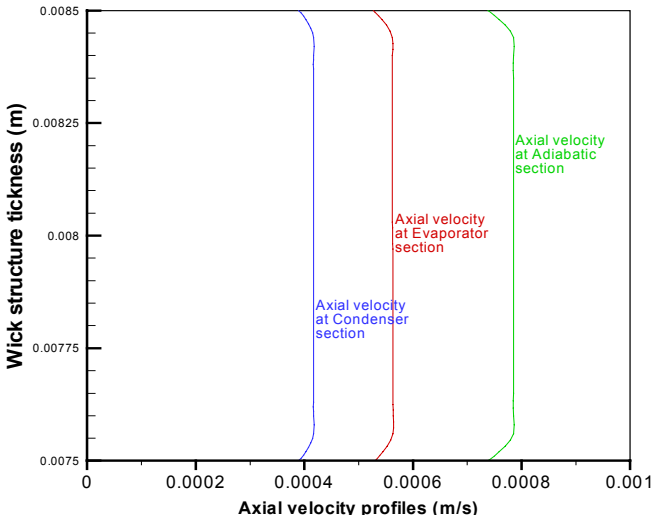

Figure 7 – Axial velocity profiles at the middle of the evaporator, adiabatic and condenser section in the wick structure

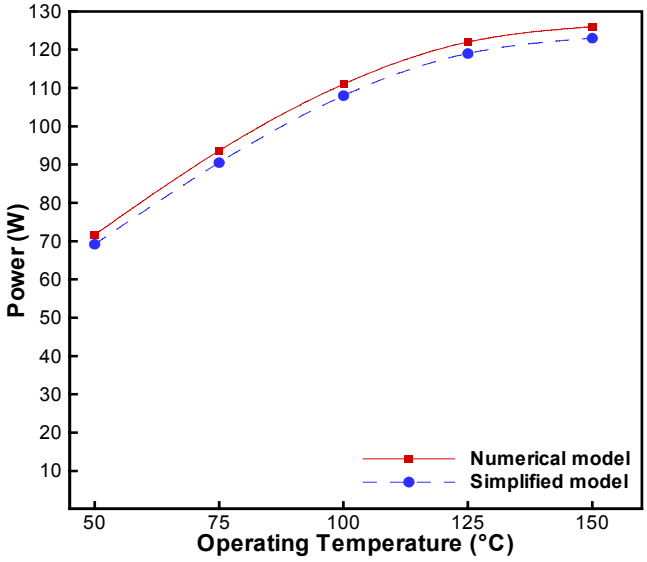

Figure 8 – Capillary limit of the Heat Pipe

This curve is very useful for the design of heat pipes. One of these curves was obtained from the numerical model described in this paper and the other with a simplified model equaling the capillary pressure with the pressure drop considering only the Darcy term and using the following equation:

$$Q = \frac{4\pi R_0 K t_w}{L_{eff} r_c} \frac{\sigma \rho_l h_{fg}}{\mu_l} \qquad (17)$$

where $L_{eff} = 0.5 L_e + L_a + 0.5 L_c$ (Peterson [15]). The vapor was assumed to be an ideal gas. Thus, the pressure and temperature are related through the equation of state for an ideal gas. As was pointed out above, the pressure drop in the vapor is very small so the vapor is almost isothermal. The capillary limit curve can be calculated numerically increasing the heat input (input blowing and suction velocities) until the failing condition is reached at the specific saturation condition. The failing condition is calculated matching the sum of the pressure drop in the vapor plus the pressure drop in the liquid with the maximum capillary pressure available at current saturation condition. The procedure is repeated for different saturation conditions. For the present conditions, the simplified model is a very good approximation in an agreement of a 3 %. The procedure mentioned above is followed to obtain the curve experimentally. However, it is important to note that to obtain this curve experimentally, it demands and requires a very good control of the heat sink in the condenser to obtain the desired operating temperature. As seen from Figure 8, the transport capacity of a heat pipe is strongly affected by changes in the thermophysical properties of the working fluid with the temperature that determine the pressure drop in the wick and the maximum capillary pressure.

Figure 9 shows the pressure drop in the liquid for three different lengths of the evaporator and condenser and the same total heat input of 85 W and a saturation condition T_{sat}=100 °C. The longer the condenser, the more recovering of the pressure and smaller pressure drop in the wick, thus improve the performance of the heat pipe. In drilling processes, the length of the evaporator is determined from the heat flux distribution near the cutting zone and has little control. On the other hand, the length of the condenser can be controlled by changing the length in contact with the holder of the drill. As it was mentioned above, the actual pressure is the sum of the reduced pressure plus the centrifugal and gravitational contribution. The gravitational contribution cannot be ignored in non-horizontal pipe and is included adding the term $\rho_l g h$ to the reduced pressure calculated from the numerical model.

Another important parameter to increase the capillary limit is the thickness of the weak structure. Figure 10 shows the pressure drop along the liquid in the wick for three different thickness of the porous medium: 1 mm, 1.5 mm and 2 mm and the same dimension of the vapor core. Increasing the thickness, the cross section for the liquid is increases and the axial velocity and the pressure drop is decreased by a similar factor that the cross sectional area. This will generate a higher temperature drop in the wick and consequently a higher superheat liquid. For rotating heat pipes, the pressure increases quadratically in the radial direction due to the effect of the centrifugal acceleration. This effect can contribute to retard the boiling limit in the evaporator allowing higher temperature drop in the porous medium and a thicker wick that improves in this way the performance of the heat pipe.
The effect of the porosity is very clear from Equation (14). The smaller the porosity, the larger the input velocities, for a

given heat flux. However, for very small velocity field in the liquid, if the convection and diffusion terms in Equation (7) are negligible, the pressure drop will be independent of the

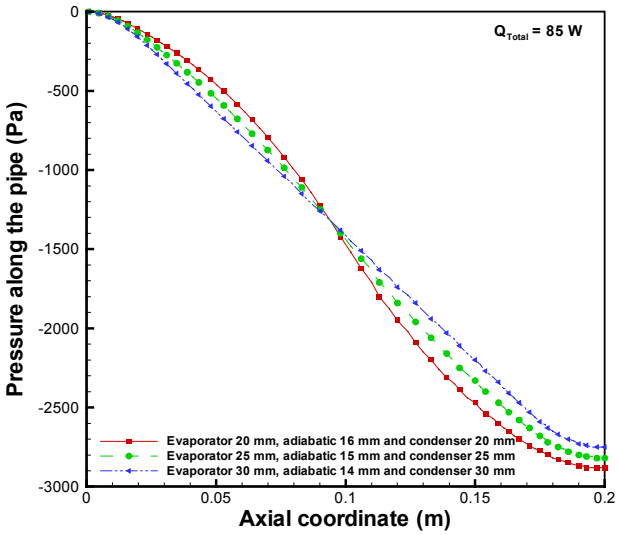

Figure 9 – Pressure drop along the heat pipe for different evaporator and condenser lengths

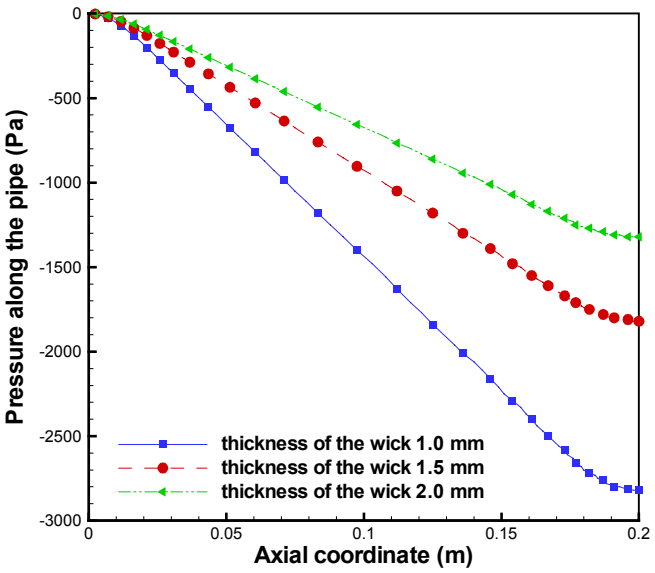

Figure 10 – Pressure drop along the heat pipe for different thickness of the wick structure

porosity. The pressure drop will be strongly influences by changes in the permeability K. By increasing K, the pressure drop wills decreases. The velocities start departing from the Darcy flow and the simplified model is no longer a good approximation. It is important to note, however, that the permeability and the porosity of the wick are related either analytically or empirically, thus changes in one of these parameters imply changes in the other.

CONCLUSIONS

A numerical model has been developed for the flow in an axially rotating heat pipe, solving the Navier-Stokes equation in the vapor core and the space-averaged of the Navier-Stokes equations in the wick structure. The capillary limit was obtained for different saturation conditions. The transport capacity is strongly affected by changes in the thermo physical properties of the working fluid with the temperature. The rotating speeds have strong effect in the vapor core but not in the liquid flow of the wick structure. However, vapor pressure drop in the vapor is very small in comparison to the pressure drop in the liquid. For the order of Reynolds number tested in this study, which is the order expected in drilling applications, the capillary limit is completely determined by the pressure drop in the wick structure. The longer the condenser, the more recovery of the pressure and smaller pressure drop in the wick are expected. Permeability, porosity and the thickness of the wick structure strongly influence the capillary limit. The rotational speed can contribute to retard the boiling limit in the evaporation allowing higher temperature drop in the porous medium and a thicker wick structure.

AKNOWLEDGEMENT

Dr. Tien-Chien Jen and Dr. Gustavo Gutierrez would like to thank the National Science Foundation (through NSF-GOALI DMII-9908324), Lamb Technicon Machining Systems and UW System Applied Research Award for their financial support of the project. The authors also like to thank Dr. Milovan Peric for providing some computer codes via Internet and Dr. Mohsen Abou-Ellail for his comments and interest in this work.

REFERENCES

[1] Bear, J., Dynamics of Fluids in Porous Media, Dover Publications, Inc., New York (1988)
[2] Ballback, L., The Operation of a Rotating Wickless Heat Pipe, M.Sc. Thesis, Monterrey, CA, U.S. Naval Postgraduate School (Ad 701674), (1969).
[3] Chew, J.W., Development of a Computer program for the Prediction of Flow in a Rotating Cavity. International Journal for Numerical Methods in Fluids, Vol. 4, 667-683 (1984)
[4] Daley, T., The Experimental Design and Operation of a Rotating Wickless Heat Pipe, M.Sc. Thesis, Monterrey, CA, U.S. Naval Postgraduate School (Ad 709923), (1970).
[5] Daniels, T. and Al-Jumaily, F., Investigation of the Factor Affecting the Performance of a Rotating Heat Pipe, Int. J. Heat Mass Transfer, Vol. 18, pp. 961-973 (1975).
[6] Ferziger J.H. and Peric M., Computational Methods for Fluid Dynamics, Springer-Verlag, Berlin, Heidelberg (1996).

[7] Faghri, A., Heat Pipe Science and Technology, Taylor & Francis, Washington, D.C (1995).
[8] Faghri,A. Gogineni, S. and Thomas, S., Vapor Flow analysis of an axially rotating heat pipe, Int. J. Heat Mass Transfer, Vol. 36, pp. 2293-2303 (1993) .
[9] Gray, V., The Rotating Heat pipe-a wickless, hollow shaft for transferring high heat fluxes, Asme-AIChE Heat Transfer Conference, Minneapolis, Minnesota (1969).
[10] Gosman, A.D. and Ideriah J.F., TEACH-T: a general computer program for two dimensional turbulent recirculating flow, in Calculation of recirculating flows, Dept. of Mech. Eng., Imperial College, University of London (1976)
[11] Harley, C. and Faghri, A., Two-Dimensional Rotating Heat Pipe Analysis, ASME J. Heat Transfer, Vol. 117, No. 1, pp. 202-208 (1995).
[12] Issacci, F., Catton, I. And Ghoniem, N.M., Vapor Dynamics of heat pipe start-up, ASME J. Heat Transfer, Vol. 113, pp. 985-994 (1991).
[13] Khosla, P.K. and Rubin, S.G., A diagonally second order accurate implicit scheme, Computers Fluids, 2, 207-209 (1974)
[14] Patankar, S.V., Numerical Heat Transfer and Fluid Flow. Hemisphere Publishing Corp., Washington, D.C (1980).
[15] Peterson, G.P., An introduction to Heat Pipes: Modeling, Testing, and Applications, Wiley, New York (1994).
[16] Peterson, G.P. and Wu, D., A Review of Rotating and Revolving Heat Pipes, ASME paper, National Heat Transfer Conference, Minneapolis, MN (1991).
[17] Sobhan, C.B., Garimella, S.V. and Unnikrishnan, V.V., A computational model for the transient analysis of flat heat pipes, ASME paper, International Heat Transfer Conference, Orlando, FL (2000).
[18] Van der Vost, H.A., BI-CGSTAB: a fast and smoothly converging variant of BI-CG for the solution of non-symmetric linear systems. SIAM J. Sci.Stat. Comput., 13, 631-644 (1992).
[19] Van Doormal, J.P. and Raithby, G.D., Enhancements of the SIMPLE method for predicting incompressible fluid flows. Numerical Heat Transfer, 7, 147-163 (1984).